

## Supporting Information

# Electron tomography resolves a complex and novel crystal structure in a nanocrystal assembly

*Mark P. Boneschanscher,<sup>1,‡</sup> Wiel H. Evers,<sup>1,‡,†</sup> Weikai Qi,<sup>2</sup> Johannes D. Meeldijk,<sup>3</sup> Marjolein Dijkstra,<sup>2</sup> and Daniel Vanmaekelbergh<sup>1,\*</sup>*

<sup>1</sup> Condensed Matter and Interfaces, Debye Institute for Nanomaterials Science, University Utrecht, Princetonplein 1, 3584 CC Utrecht, The Netherlands; <sup>2</sup> Soft Condensed Matter, Debye Institute for Nanomaterials Science, University Utrecht, Princetonplein 1, 3584 CC Utrecht, The Netherlands; <sup>3</sup> Electron Microscopy Group, Utrecht University, Padualaan 8, 3584 CH Utrecht, The Netherlands.

‡ These authors contributed equally.

† Present address: Kavli Institute of NanoScience, Delft University of Technology, Faculty of Applied Sciences, Lorentzweg 1, 2628 CJ Delft, The Netherlands.

## Table of content

- I Details on the NC synthesis and the computer aided particle detection
- II Various TEM images of crystal structures observed at a size ratio range of 0.61-0.67
- III Unit cell parameters of the  $A_6B_{19}$  crystal structure
- IV Space group assignment of the  $A_6B_{19}$  crystal structure
- V Monte-Carlo simulation of the  $A_6B_{19}$  crystal structure
- VI References

## **I Details on the NC synthesis and the computer aided particle detection**

Oleic acid capped PbSe and trioctylphosphine oxide/hexadecylamine capped CdSe NC were prepared according to literature.<sup>1,2</sup> The as prepared NCs had an inorganic core size of  $6.5\pm 0.4$ nm (PbSe) and  $3.4\pm 0.3$ nm (CdSe) and an effective size of  $9.4\pm 0.3$ nm (PbSe) and  $5.8\pm 0.3$ nm (CdSe). Effective sizes, giving an estimate for the contribution of the soft ligand shell, were determined by measuring the centre-to centre distance of the NCs in a hexagonally packed single-component monolayer.

The NCSL were prepared by solvent evaporation as reported previously.<sup>3</sup> In short, suspensions of the PbSe and CdSe NCs in tetrachloroethylene were mixed at concentration ratio of 1:4 PbSe:CdSe. Colloidal crystallization was achieved by evaporation of the solvent under reduced pressure ( $\sim 10$  mbar) and enhanced temperature ( $70$  °C) while keeping the substrate (a Pioloform coated TEM-grid) under an angle of  $30^\circ$  to the horizon. All synthesis were performed in a nitrogen purged glovebox.

Electron tomography was performed in a similar way as described in depth in previous work.<sup>4</sup> Transmission images and tilt series were acquired in bright-field mode using a Tecnai 20 electron microscope with a LaB<sub>6</sub> electron source (FEI Company, Eindhoven). The tilt series were acquired over  $\pm 65^\circ$  with a  $1^\circ$  increment. The entire object was imaged in underfocus throughout the tilt series.

Particle detection was done using template matching in Matlab as described by Heiner et al.<sup>4</sup> Following on the particle detection a statistical analysis of the unit cell was performed. The unit vectors were determined by averaging over the nearest neighbor distances that were determined by a Voronoi analysis. Particle positions were then expressed as a distance from the origin of their respective unit cells. Averaging over these distances resulted in the final coordinates. Since the spread in the CdSe positions was very large we used an additional detection criterion. This was to only include positions that were separated over at least one CdSe diameter (inorganic core diameter) from other CdSe positions within the same unit cell.

## II Various TEM images of crystal structures observed at a size ratio range of 0.61-0.67

For self-assembly of the NCs at a size ratio range of 0.61-0.67 various structures are observed that show long-range ordering (Figure S1). Although the grain size of the structures can go up to several micrometers, a lot of different structures are observed within 1 synthesis. An overview of some typical crystal structures/orientations observed on one TEM grid is shown in Figure S2.

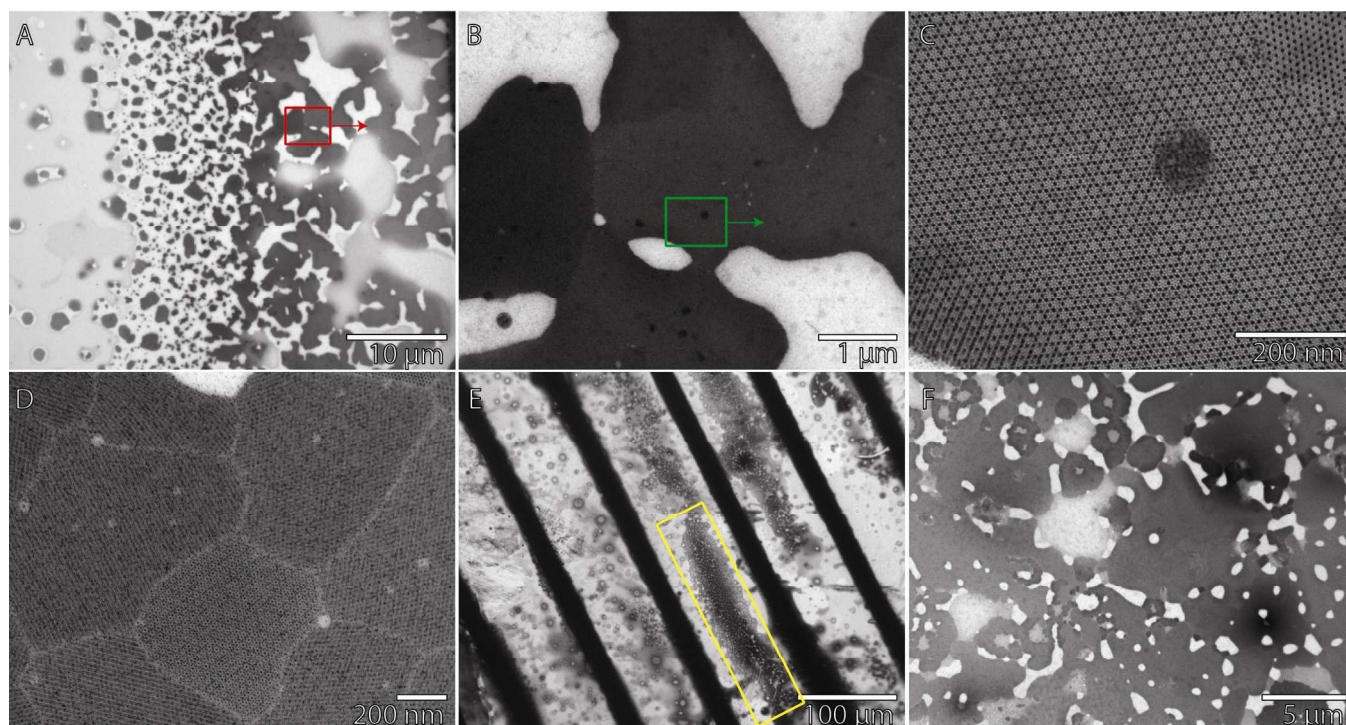


**Figure S1.** Typical overview TEM images of self-assembled NC superlattices in the size ratio of 0.61-0.67. (a-c) Various TEM images of the same region showing micrometer sized single domains of various crystal structures/orientations. (b) Zoom in on the red square in (a). (c) Zoom in on the green square of (b). (d) Various crystal domains with small grain sizes. (e) Large scale overview, where the region of the crystallites shown in (d) is indicated with the yellow box. (f) Zoomed in TEM image of (e) showing crystallites (dark patches) next to thin disordered regions (bright patches). Note that the average overall surface coverage of the various crystal structures in this size ratio is <1%

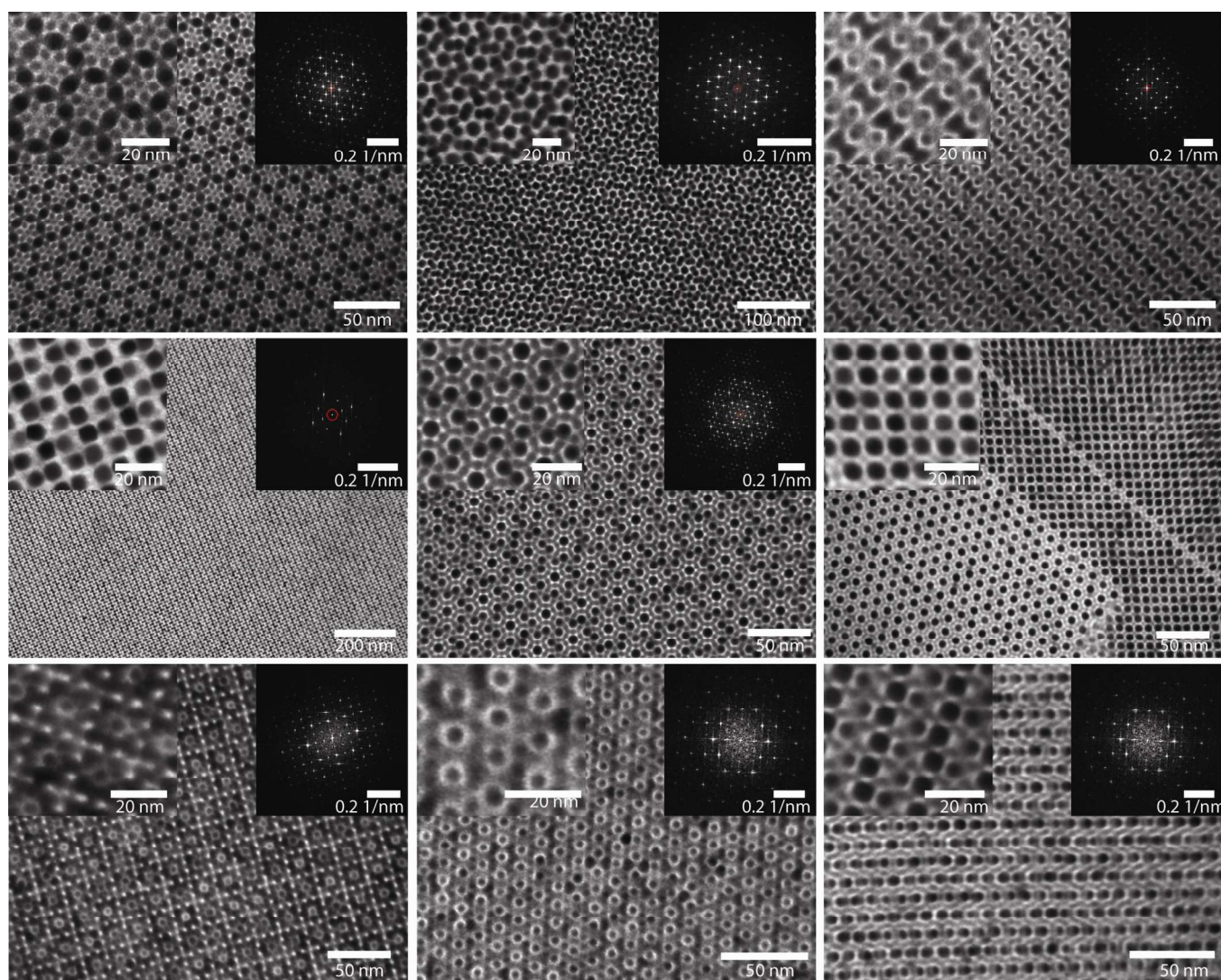


**Figure S2.** TEM images of (unknown) binary nanocrystal superlattices/orientations observed in the size ratio range 0.61-0.67. In the inset the FFT of the obtained superlattices is given. All structures are observed on one and the same TEM grid. The very first panel shows the TEM image of the structure discussed in the paper.

### III Unit cell parameters of the $A_6B_{19}$ crystal structure

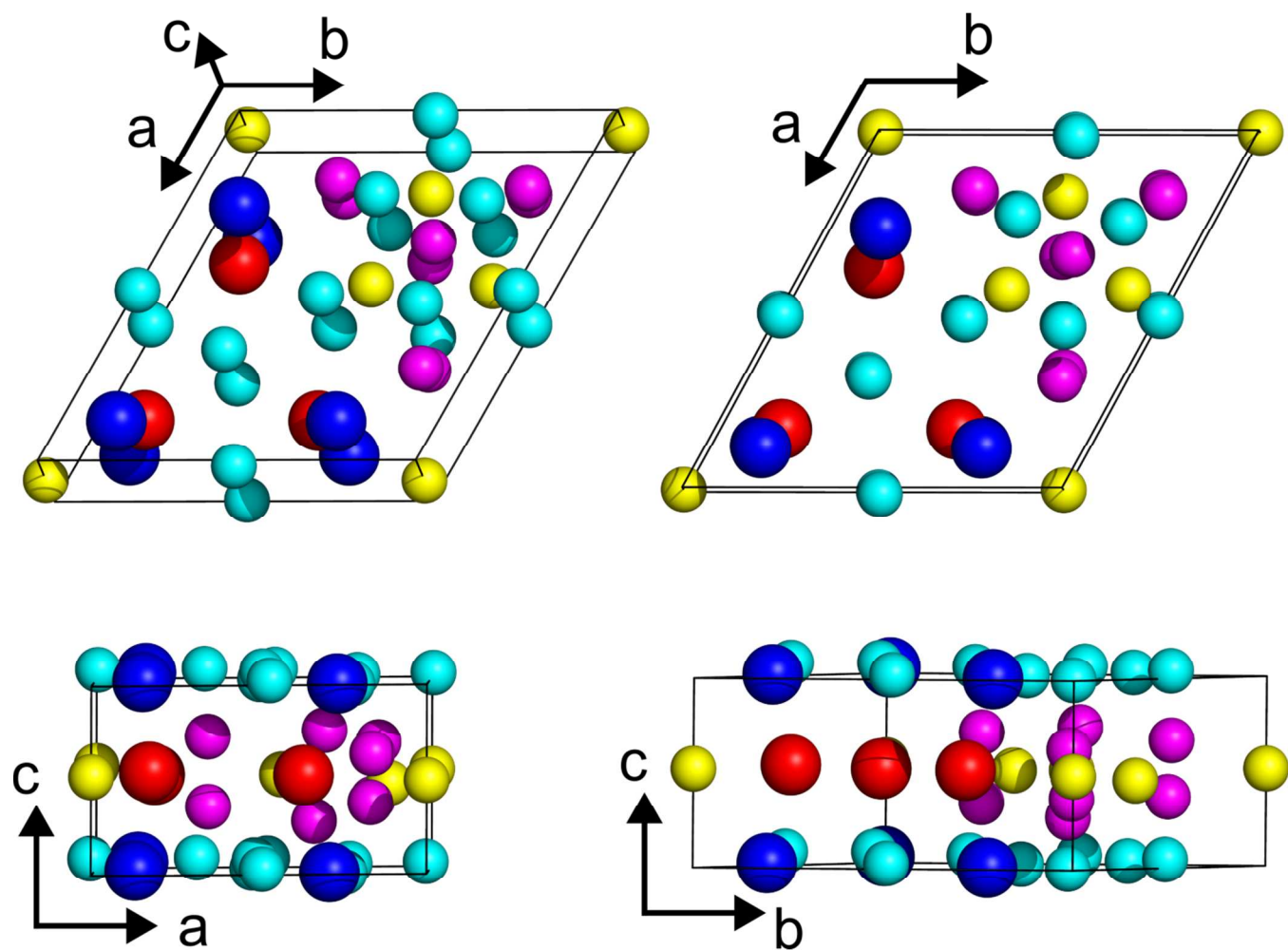


**Figure S3.** Three dimensional, top and different side views of the detected unit cell. Balls with the same color depict nanocrystals within the same layer. PbSe nanocrystals are displayed in blue and red, CdSe nanocrystals in cyan, magenta and yellow. The unit vectors are defined as **a** in the xy plane at an angle of  $-120^\circ$  with the x-axis, **b** along the x-axis and **c** along the z-axis.

**Table S1.** Lattice parameters given in Cartesian coordinates, lengths and angles.

Unit vector	x (nm)	y (nm)	z (nm)	Length (nm)	Angle ( $^\circ$ )
<b>a, <math>\alpha</math></b>	$-9.4 \pm 0.7$	$-22.3 \pm 0.6$	$-0.2 \pm 0.8$	$24.2 \pm 0.7$	$89.2 \pm 2.8$
<b>b, <math>\beta</math></b>	$22.4 \pm 0.7$	$2.3 \pm 0.8$	$-0.3 \pm 0.7$	$22.5 \pm 0.7$	$89.4 \pm 1.8$
<b>c, <math>\gamma</math></b>	$0.3 \pm 0.9$	$-0.4 \pm 0.9$	$11.2 \pm 0.7$	$11.2 \pm 0.8$	$118.7 \pm 2.5$

**Table S2.** The 25 unique nanocrystal positions within the unit cell given in both Cartesian coordinates and fractions of the unit vectors. Color coding refers to Figure S3.

Nanocrystal	x (nm)	y (nm)	z (nm)	a	b	c
<b>PbSe (blue)</b>	$-5.1 \pm 0.7$	$-19.3 \pm 0.9$	$-0.2 \pm 0.9$	$0.88 \pm 0.03$	$0.14 \pm 0.04$	$0.00 \pm 0.08$
<b>PbSe (blue)</b>	$7.9 \pm 0.7$	$-18.0 \pm 0.9$	$-0.4 \pm 0.6$	$0.88 \pm 0.03$	$0.72 \pm 0.04$	$0.00 \pm 0.05$
<b>PbSe (blue)</b>	$0.6 \pm 1.0$	$-5.7 \pm 0.7$	$0.0 \pm 0.6$	$0.27 \pm 0.04$	$0.14 \pm 0.03$	$0.01 \pm 0.05$
<b>PbSe (red)</b>	$6.5 \pm 1.0$	$-17.3 \pm 0.9$	$5.4 \pm 0.9$	$0.83 \pm 0.04$	$0.63 \pm 0.04$	$0.51 \pm 0.08$
<b>PbSe (red)</b>	$0.6 \pm 1.2$	$-8.3 \pm 0.9$	$5.2 \pm 0.9$	$0.38 \pm 0.05$	$0.18 \pm 0.04$	$0.48 \pm 0.08$
<b>PbSe (red)</b>	$-3.8 \pm 1.2$	$-18.3 \pm 1.1$	$5.6 \pm 1.0$	$0.83 \pm 0.05$	$0.17 \pm 0.05$	$0.52 \pm 0.09$
<b>CdSe (cyan)</b>	$0.8 \pm 1.0$	$-14.5 \pm 0.7$	$0.4 \pm 0.9$	$0.68 \pm 0.04$	$0.32 \pm 0.03$	$0.06 \pm 0.08$
<b>CdSe (cyan)</b>	$6.1 \pm 1.0$	$-10.5 \pm 0.7$	$0.2 \pm 0.9$	$0.52 \pm 0.04$	$0.49 \pm 0.03$	$0.04 \pm 0.08$
<b>CdSe (cyan)</b>	$12.2 \pm 1.0$	$-10.7 \pm 0.7$	$10.6 \pm 0.4$	$0.54 \pm 0.04$	$0.76 \pm 0.03$	$0.98 \pm 0.04$
<b>CdSe (cyan)</b>	$-4.8 \pm 1.0$	$-11.4 \pm 0.7$	$0.3 \pm 0.7$	$0.51 \pm 0.04$	$0.00 \pm 0.03$	$0.04 \pm 0.06$
<b>CdSe (cyan)</b>	$8.9 \pm 1.2$	$-4.4 \pm 0.7$	$10.8 \pm 0.7$	$0.23 \pm 0.05$	$0.48 \pm 0.03$	$0.98 \pm 0.06$
<b>CdSe (cyan)</b>	$14.9 \pm 1.0$	$-3.8 \pm 0.9$	$-0.2 \pm 0.7$	$0.25 \pm 0.04$	$0.77 \pm 0.04$	$0.01 \pm 0.06$
<b>CdSe (cyan)</b>	$11.6 \pm 1.2$	$1.0 \pm 0.7$	$0.1 \pm 1.0$	$0.01 \pm 0.05$	$0.52 \pm 0.03$	$0.02 \pm 0.09$
<b>CdSe (magenta)</b>	$11.6 \pm 0.7$	$-6.4 \pm 0.7$	$2.4 \pm 0.4$	$0.35 \pm 0.03$	$0.66 \pm 0.03$	$0.24 \pm 0.04$
<b>CdSe (magenta)</b>	$6.1 \pm 1.0$	$-3.1 \pm 0.7$	$3.2 \pm 0.8$	$0.17 \pm 0.04$	$0.34 \pm 0.03$	$0.30 \pm 0.07$
<b>CdSe (magenta)</b>	$12.4 \pm 1.0$	$-13.2 \pm 0.7$	$3.6 \pm 0.9$	$0.67 \pm 0.04$	$0.83 \pm 0.03$	$0.36 \pm 0.08$
<b>CdSe (magenta)</b>	$17.1 \pm 1.0$	$-2.0 \pm 0.7$	$3.6 \pm 0.9$	$0.17 \pm 0.04$	$0.83 \pm 0.03$	$0.35 \pm 0.08$
<b>CdSe (yellow)</b>	$0.2 \pm 1.0$	$-0.2 \pm 1.1$	$5.6 \pm 1.1$	$0.00 \pm 0.04$	$0.00 \pm 0.05$	$0.50 \pm 0.10$
<b>CdSe (yellow)</b>	$8.6 \pm 0.7$	$-8.7 \pm 0.4$	$5.2 \pm 0.4$	$0.44 \pm 0.03$	$0.56 \pm 0.02$	$0.49 \pm 0.04$
<b>CdSe (yellow)</b>	$11.4 \pm 1.0$	$-2.9 \pm 0.7$	$5.2 \pm 0.4$	$0.18 \pm 0.04$	$0.58 \pm 0.03$	$0.48 \pm 0.04$
<b>CdSe (yellow)</b>	$15.7 \pm 1.0$	$-8.0 \pm 1.1$	$4.7 \pm 0.7$	$0.44 \pm 0.04$	$0.88 \pm 0.05$	$0.45 \pm 0.06$
<b>CdSe (magenta)</b>	$12.3 \pm 1.0$	$-6.3 \pm 0.9$	$7.8 \pm 0.6$	$0.34 \pm 0.04$	$0.68 \pm 0.04$	$0.72 \pm 0.05$
<b>CdSe (magenta)</b>	$6.1 \pm 1.2$	$-3.1 \pm 0.9$	$7.4 \pm 0.8$	$0.16 \pm 0.05$	$0.33 \pm 0.04$	$0.67 \pm 0.07$
<b>CdSe (magenta)</b>	$12.3 \pm 1.0$	$-13.7 \pm 0.7$	$6.6 \pm 0.7$	$0.69 \pm 0.04$	$0.83 \pm 0.03$	$0.62 \pm 0.06$
<b>CdSe (magenta)</b>	$17.3 \pm 1.0$	$-2.3 \pm 0.7$	$7.0 \pm 0.6$	$0.18 \pm 0.04$	$0.84 \pm 0.03$	$0.65 \pm 0.05$

## IV Space group assignment of the $A_6B_{19}$ crystal structure

To assign the correct space group to the  $A_6B_{19}$  crystal structure the programme FINDSYM<sup>5</sup> was used. The unit vectors as given in Table S1 and the positions as given in Table S2 were used as input. As additional input parameters we used a tolerance of 1.7nm, a random centering and an hexagonal axes system. Using these tolerance settings, the symmetry operations possible showed that the  $A_6B_{19}$  structure can be classified in the  $P\bar{6}m2$  space group (no. 187). Forcing this symmetry upon the structure, the occupation of the unit cell can be given in Wyckoff positions (Table S3).

**Table S3.** The nanocrystal positions within the unit cell when forcing  $P\bar{6}m2$  symmetry. The unit cell vectors are  $\mathbf{a} = \mathbf{b} = 23.36\text{nm}$ ,  $\mathbf{c} = 11.21\text{nm}$  with  $\alpha = \beta = 90^\circ$  and  $\gamma = 120^\circ$ . Color coding refers to Figure S3.

Nanocrystal	<b>a</b>	<b>b</b>	<b>c</b>
<b>Wyckoff position j, x = -0.135</b>			
<b>PbSe (blue)</b>	0.270	0.135	0.000
<b>PbSe (blue)</b>	0.865	0.135	0.000
<b>PbSe (blue)</b>	0.865	0.730	0.000
<b>Wyckoff position k, x = -0.182</b>			
<b>PbSe (red)</b>	0.363	0.182	0.500
<b>PbSe (red)</b>	0.818	0.182	0.500
<b>PbSe (red)</b>	0.818	0.637	0.500
<b>Wyckoff position e</b>			
<b>CdSe (cyan)</b>	0.667	0.333	0.000
<b>Wyckoff position j, x = -0.497</b>			
<b>CdSe (cyan)</b>	0.503	0.007	0.000
<b>CdSe (cyan)</b>	0.503	0.497	0.000
<b>CdSe (cyan)</b>	0.993	0.497	0.000

<b>Wyckoff position j, x = 0.237</b>			
CdSe (cyan)	0.237	0.473	0.000
CdSe (cyan)	0.237	0.763	0.000
CdSe (cyan)	0.572	0.763	0.000
<b>Wyckoff position h, z = -0.260</b>			
CdSe (magenta)	0.333	0.667	0.260
CdSe (magenta)	0.333	0.667	0.740
<b>Wyckoff position n, x = 0.166, z = -0.345</b>			
CdSe (magenta)	0.166	0.332	0.345
CdSe (magenta)	0.166	0.834	0.345
CdSe (magenta)	0.668	0.834	0.345
CdSe (magenta)	0.166	0.332	0.655
CdSe (magenta)	0.166	0.834	0.655
CdSe (magenta)	0.668	0.834	0.655
<b>Wyckoff position b</b>			
CdSe (yellow)	0.000	0.000	0.500
<b>Wyckoff position k, x = 0.430</b>			
CdSe (yellow)	0.140	0.570	0.500
CdSe (yellow)	0.430	0.570	0.500
CdSe (yellow)	0.430	0.860	0.500

Comparing the measured crystal structure with the structure after forcing  $P\bar{6}m2$  symmetry we note that, in order to force the  $P\bar{6}m2$  symmetry we had to move the particles over distances that fall well below the standard deviation in our measurement as presented in Table S2 (see also Figure S4). We therefore conclude that the deviation of the measured crystal structure from  $P\bar{6}m2$  symmetry is more likely to be a measurement error than a physical phenomenon.

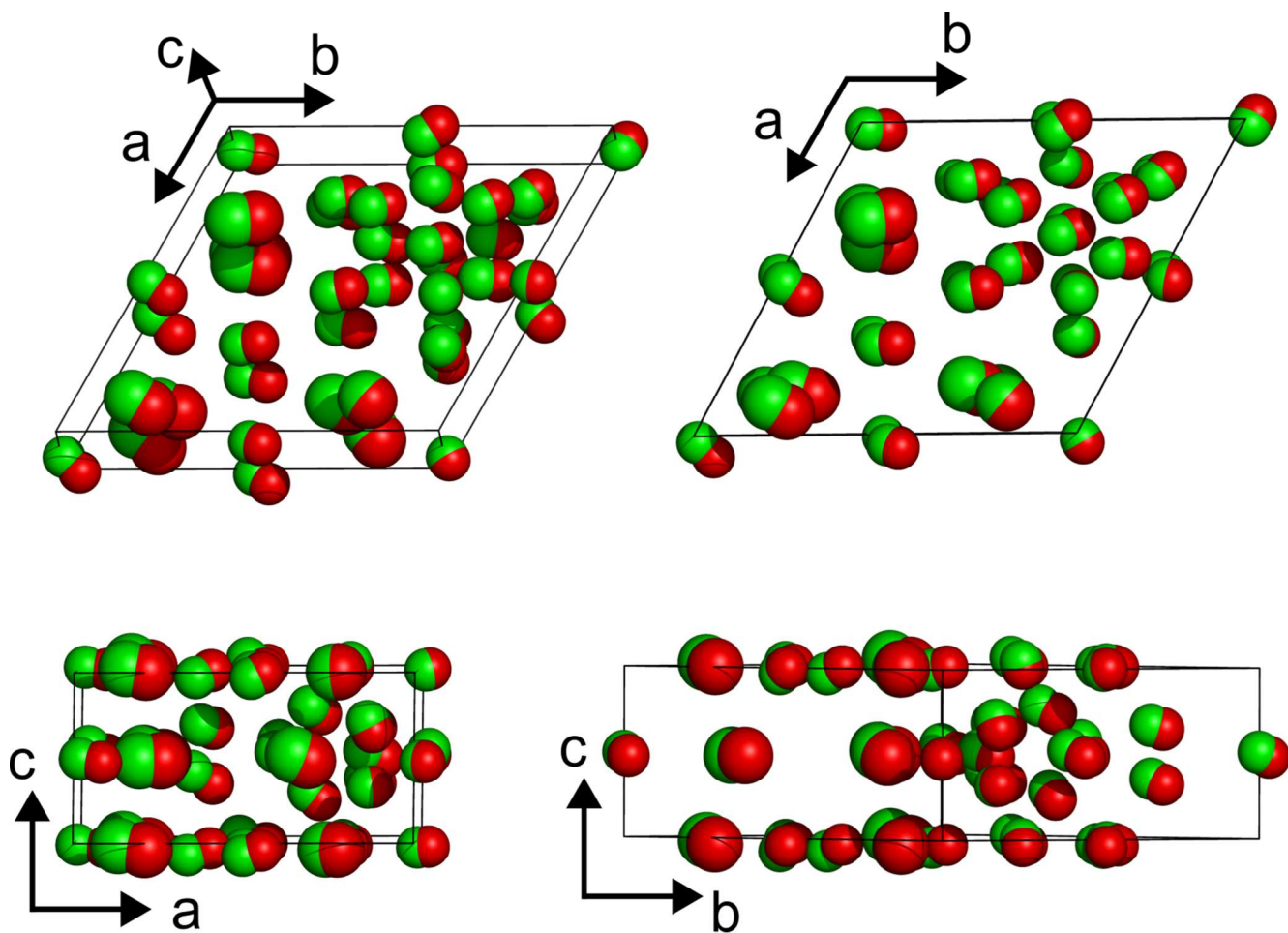


**Figure S4.** Comparison of the detected unit cell before (green) and after (red) forcing  $P\bar{6}m2$  symmetry. Note that the balls are not drawn to scale. The shift in position in order to force  $P\bar{6}m2$  symmetry is well below the standard deviation of the measured positions.

## V Monte Carlo simulation of the $A_6B_{19}$ structure

To evaluate whether the experimentally observed  $A_6B_{19}$  structure is stable for a binary mixture of hard spheres, Monte Carlo (MC) simulations were performed (Figure S5a). The configuration of the experimental results and a size ratio of 0.695 were used as initial parameters for the simulations. Subsequently the system was compressed to a higher pressure of  $PV/kT= 1000000.0$  using 300000 MC steps. The densest packing fraction obtained in our simulation is 0.641. Although this is higher than the experimental values for the inorganic cores only, it is still much below the 0.85 we find with the effective sizes. Figure S5b shows the densest structure obtained in our simulations. Compared to the experimental configuration, some of the small particles moved out of position and the structure becomes more disordered. If the particles are only allowed to move in the xy direction, the  $A_6B_{19}$  structure seems to be stable. The maximum packing fraction obtained in this case is 0.575.

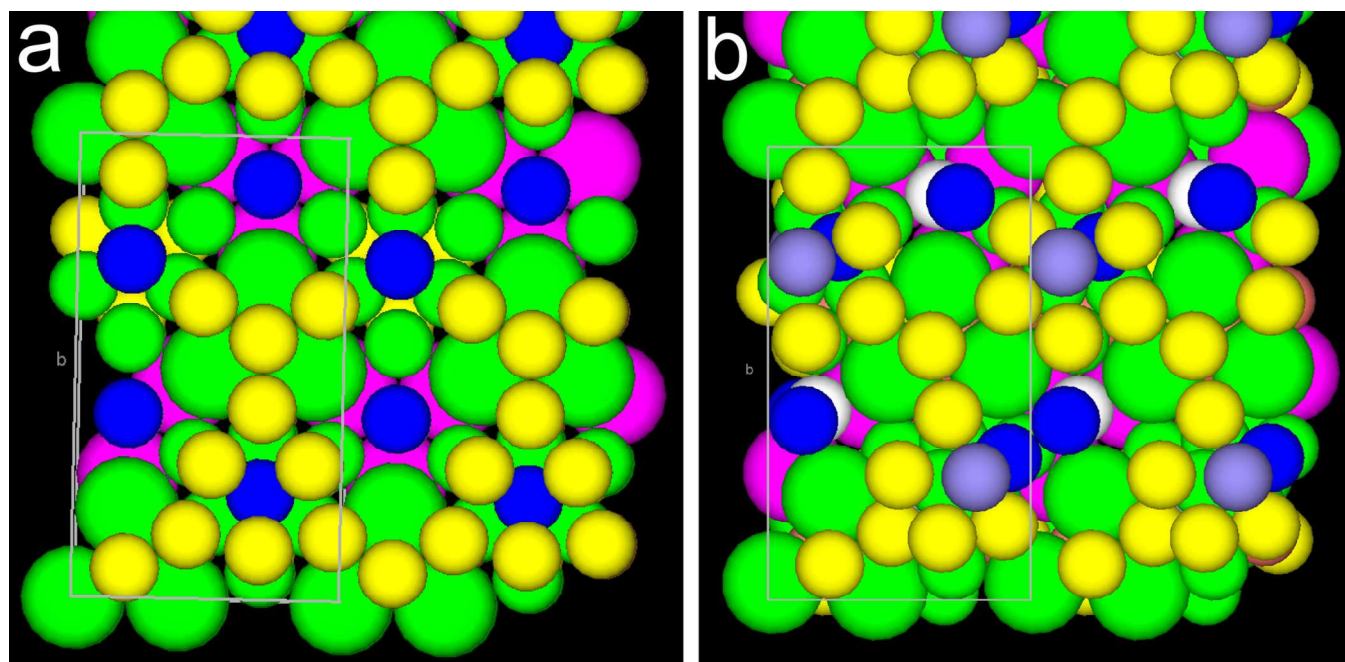


**Figure S5.** (a) Top view of the  $A_6B_{19}$  initial configuration obtained from experiment. The color coding of the particles corresponds to the particular height of their center of mass. (b) Densest packing structure obtained by MC simulations.

To assess the crystal structures and densest packing fraction at various size ratios in a range of 0.61-0.72, floppy box simulations were performed on 25 particles (6 large and 19 small particles) in a unit cell.<sup>6</sup> In floppy box simulations, the shape of the unit cell is allowed to vary in order to fit the possible crystal structures. After 100 independent simulations we observed a variation of the densest packing fraction in the range of 0.668-0.686 as a function of size ratio (Figure S6). However, due to the amount of particles in the unit cell (25), the particles packed into a disordered jammed structure as for example given in Figure S7.

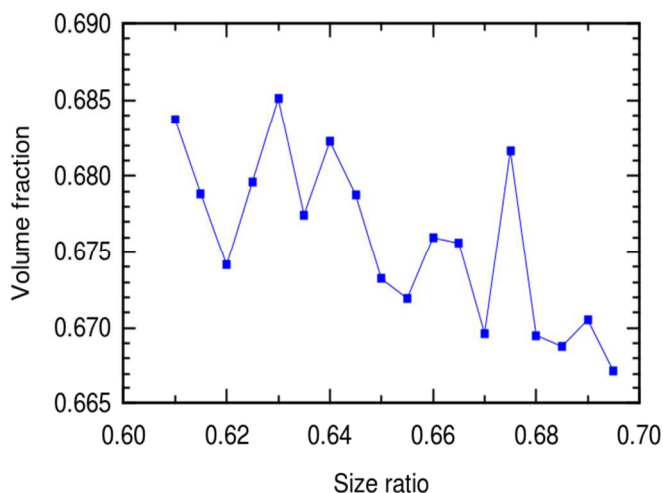


**Figure S6.** Densest obtained volume fraction as a function of particle size ratio.

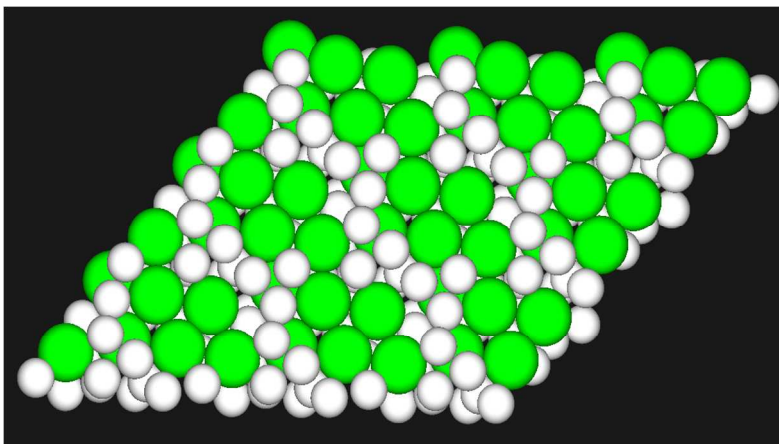


**Figure S7.** Disordered packed structures obtained by floppy box simulations. The PbSe positions are indicated in green and the CdSe positions in white.

Our finding that MC simulations with hard spheres are unable to reproduce the experimentally found structure can be attributed to complications in the modelling due to the large system size. On the other hand, this finding may point out that the system actually cannot be modelled with hard spheres anymore. This would imply that the formation of the observed crystal structure cannot be explained by entropy alone. If this is true, than it would be counterintuitive with our earlier work<sup>3</sup> where we describe how, for exactly the same nanocrystals and the same chemical environment, we mainly do find superlattice structures of which the formation can be explained with entropy only. We would like to point out however, that in the size ratio regime of 0.61-0.67 used in this study, no stable structures of hard spheres have been predicted. As such, the formation of the crystal structure described in this work does not need to compete with entropy driven crystallization. Therefore we do not think that the enthalpic interaction between the nanocrystals necessarily needs to be large to explain the observed superlattice crystal structure. Rather, we think that enthalpy plays a bigger role in this superlattice crystal formation, simply due to the lower entropic contribution.

In order to find out if enthalpic interactions would stabilize the observed crystal structure, further research is necessary. A MC study of the system using slightly attractive and repulsive potentials between the particles would be recommendable, but falls beyond the scope of the present work. More detailed modelling of the system will however be complicated since the overall interaction potential between the NCs will be influenced by, among others, steric hindrance of the capping ligands, (screened) Van der Waals interaction between the NCs and residual charges on the NC surface or in solution.

## VI References

- (1) Houtepen, A. J.; Koole, R.; Vanmaekelbergh, D.; Meeldijk, J.; Hickey, S. G. *J. Am. Chem. Soc.* **2006**, *128*, 6792-6793.
- (2) de Mello Donegá, C.; Hickey, S. G.; Wuister, S. F.; Vanmaekelbergh, D.; Meijerink, A. *J. Phys. Chem. B* **2003**, *107*, 489-496.
- (3) Evers, W. H.; de Nijs, B.; Filion, L.; Castillo, S.; Dijkstra, M.; Vanmaekelbergh, D. *Nano Lett.* **2010**, *10*, 4235–4241.
- (4) Friedrich, H.; Gommès, C. J.; Overgaag, K.; Meeldijk, J. D.; Evers, W. H.; de Nijs, B.; Boneschanscher, M. P.; de Jongh, P. E.; Verkleij, A. J.; de Jong, K. P.; van Blaaderen, A.; Vanmaekelbergh, D. *Nano Lett.* **2009**, *9*, 2719–2724.
- (5) Stokes, H. T.; Campbell, B. J.; Hatch, D. M.; *FINDSYM*, [stokes.byu.edu/iso/findsym.html](http://stokes.byu.edu/iso/findsym.html) **2013**.
- (6) Filion, L.; Marechal, M.; Oorschot, B.; Pelt, D.; Smalenburg, F.; Dijkstra, M.; *Phys. Rev. Lett.* **2009**, *103*, 188302.